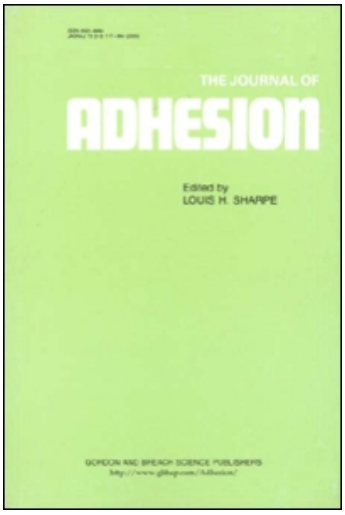

The Journal of Adhesion
Publication details, including instructions for authors and subscription information:
http://www.informaworld.com/smpp/title~content=t713453635

MEASURING INTERFACIAL ADHESION BETWEEN A SOFT VISCOELASTIC LAYER AND A RIGID SURFACE USING A PROBE METHOD

Gwendal Josse[a]; Philippe Sergot[a]; Costantino Creton[a]; Michel Dorget[b]
[a] Laboratoire de Physico-Chimie Structurale et Macromoléculaire, E.S.P.C.I., Paris, France [b] Centre de Transfert de Technologie, Le Mans, France

Online publication date: 10 August 2010

To cite this Article Josse, Gwendal , Sergot, Philippe , Creton, Costantino and Dorget, Michel(2004) 'MEASURING INTERFACIAL ADHESION BETWEEN A SOFT VISCOELASTIC LAYER AND A RIGID SURFACE USING A PROBE METHOD', The Journal of Adhesion, 80: 1, 87 — 118
To link to this Article: DOI: 10.1080/00218460490276821
URL: http://dx.doi.org/10.1080/00218460490276821

The Journal of Adhesion, 80: 87–118, 2004

ISSN: 0021-8464 print/1545-5823 online
DOI: 10.1080/00218460490276821

Taylor & Francis
Taylor & Francis Group

MEASURING INTERFACIAL ADHESION BETWEEN A SOFT VISCOELASTIC LAYER AND A RIGID SURFACE USING A PROBE METHOD

Gwendal Josse
Philippe Sergot
Costantino Creton
Laboratoire de Physico-Chimie Structurale et Macromoléculaire, E.S.P.C.I., Paris, France

Michel Dorget
Centre de Transfert de Technologie, Le Mans, France

A reliable measure of the adhesion between a very deformable material and a solid surface is rather difficult, since the interface boundary conditions and the bulk deformation of the layer are closely and very nonlinearly coupled. In this article, a new methodology to assess the adhesion of a soft viscoelastic layer on a solid surface is proposed, where we have used a specific experimental geometry minimizing the bulk deformation of the layer. A flat-ended probe is first put in contact with a thin layer of soft material and removed at a constant velocity. The probe is then stopped at a preset level of tensile force and the time for complete debonding of the layer from the probe is measured. For our model system, comprised of a soft acrylic removable adhesive and a silicone-coated surface, the higher the applied force the faster the interfacial fracture occurs, leading to an experimental curve of the adhesion energy as a function of average crack velocity. We find that the methodology is relatively simple to implement and should be widely applicable for weakly adhering soft layers of arbitrary viscoelastic properties. The assumptions involved in such an analysis and their inherent limitations are also illustrated experimentally and critically discussed.

Keywords: Silicone; Adhesion; Probe; Acrylate; PSA; Fracture; Tack

Received 23 July 2003; in final form 14 November 2003.

One of a collection of papers honoring Jacob Israelachvili, the recipient in February 2003 of *The Adhesion Society Award for Excellence in Adhesion Science, Sponsored by 3M.*

We gratefully acknowledge the financial support of Rhodia Silicones.

The current address of Gwendal Josse is Centre de Recherche Européen sur la Peau, Institut de Recherche Pierre Fabre, Centre Jean Louis Alibert, 2 rue Viguerie, BP 3071, 31025 Toulouse Cedex 3-France.

Address correspondence to Costantino Creton, Laboratoire de Physico-Chimie Structurale et Macromoléculaire, E.S.P.C.I., 10, Rue Vauquelin, 75231 Paris Cédex, France. E-mail: Costantino.Creton@espci.fr

INTRODUCTION

Reliably measuring the adhesion between soft bodies is an extremely relevant topic technologically and an interesting one scientifically. It spans several areas of research and development such as biology, food science, materials processing, and generally all areas where a soft and deformable material comes in contact with a surface.

Scientifically, the topic has been approached from two different angles depending on the nature of the soft material. Restricting ourselves to homogeneous materials, the adhesion of fluids on surfaces has been recently investigated in depth, and the standard fluid mechanics assumption of perfect adhesion with no slippage of molecules at the interface has been clearly proven wrong, at least for macromolecular entangled fluids [1]. The degree of molecular slippage at the interface has been identified as a key parameter controlling the boundary conditions of fluid flow and, hence, the level of dissipation. This surface slippage is nearly absent for small molecules but becomes an important issue for entangled polymers. Starting from a description of Newtonian polymeric fluids this concept has been shown to be relevant for soft gels as well [2].

At the other end of the spectrum, the adhesion of crosslinked elastomers on rigid surfaces has been extensively studied, mainly with the so-called JKR technique, which is based on contact mechanics theory [3–6]. In such an approach, the effect of adhesive forces is balanced by the elastic strain energy a well-defined geometry in contact. Several good reviews of this topic are readily available [7–10].

In real life, however, many materials are neither elastic nor flowing. In this case the very definition of adhesion becomes complex and one should speak of coupling between the interfacial boundary conditions and the deformation of the material instead. Such viscoelastic and highly deformable solid materials are present in pressure-sensitive adhesives [11], some inks, food, cosmetics, and a variety of more complex biological problems. In this article we will propose a methodology to characterize the adhesion of such materials to solid surfaces.

First of all, let us define the context: the word adhesion can take a variety of meanings, depending on who uses its. We will restrict ourselves here to the energy dissipated in the material during a test in which two surfaces previously in contact are separated. The crucial problem of evaluating such an adhesion energy for soft viscoleastic materials is to separate the energy which is directly related to the interface from that which is simply related to the deformation of the bulk material, independently of the surface boundary conditions.

Some progress has been made in the recent years towards a better definition of "interfacial" and "bulk" dissipation, [12]. In fact, neither dissipation mechanism is, strictly speaking, purely bulk or purely interfacial. A better definition is to associate the interfacial dissipation with the propagation of a crack front at relatively low levels of strain, which does not involve a significant degree of extension of the polymer molecules. On the other hand, the bulk dissipation is associated with little or no propagation of a crack front and with the formation of elongated fibrils where the polymer molecules are highly stretched.

Additionally, the dissipation process cannot be dissociated from a characteristic strain rate. If the dissipative processes are of viscous origin, the rate at which the deformation is applied will greatly influence the local stresses. In terms of energy, one can propose, in all generality, that the rate at which the elastic energy is released near the interface will have to be matched by the dissipation rate, corresponding to a characteristic steady-state crack velocity.

Within the framework of these definitions, our goal is to measure the "interfacial" dissipation that occurs when a soft layer is detached from a solid substrate at a given rate. Let us now discuss briefly the hypotheses that need to be made.

In the classic linear elastic fracture mechanics description, the materials behave elastically except in the immediate vicinity of the crack tip, which acts as an energy sink and where all the energy is dissipated [13]. The result of such a test is a value of $\mathcal{G}_c$, a critical energy release rate which is unambiguously related to the interface. In this case, the (elastic) loading process is effectively decoupled from the (viscoelastic or plastic) interfacial dissipation. This description applies very well to brittle or semibrittle materials such as glassy polymers. For lightly viscoleastic rubbers on solid surfaces, the length scales are no longer really separated but the times scales can be separated as discussed in a recent review paper by Unertl [9]. If the bulk material is viscoelastic but relaxes much faster in the bulk than at the interface, the loading can still be considered as elastic and the only dissipation to occur near the interface. This situation can also be called small-scale viscoelasticity. If the material is highly viscoelastic, neither the length nor the times scales are well separated so that the energy flow towards the crack tip cannot be evaluated exactly and is closely coupled to the dissipation process at the crack tip. This point was discussed extensively by Hui [14–18] and Barthel [19, 20], and has been recently reviewed by Shull [10]. This situation is defined as large-scale viscoelasticity.

In both of the previously discussed cases, the viscoelasticity in the bulk is limited to the linear regime, *i.e.*, small strains except in the

immediate vicinity of the crack tip. However, in the case of very soft materials, the crack can effectively blunt and the zone where large elongational strains occur can extent over the whole sample. In this case, it is very useful to limit the size of the sample through confinement to obtain information on the adhesion of the material to a surface rather than on its large strain behavior.

In this article, we explore how the geometry of the test can be used to limit bulk nonlinear viscoelasticity effectively and to improve the separation of the time scales of the relaxation process in the bulk from that of the dissipation at the interface. These results will then be used to evaluate an interfacial adhesion energy. We will use the example of the detachment of a typical soft, polymer-based adhesive, which is normally used as a removable pressure-sensitive adhesive, from a surface of steel and from a surface of crosslinked polydimethysiloxane, typically used as a release surface for the adhesive before use.

To perform our test, we will use a flat probe geometry, described schematically in Figure 1, which applies a high level of confinement to the layer. The confined geometry has two distinct advantages:

- because of the near incompressibility of the layer, it is possible to store much more elastic energy per unit volume in the layer than in the unconfined case before failure starts.
- The average degree of deformation is uniform laterally and is controlled by the spacing between plates. This effectively allows a control of the average degree of elongation of the chains.

If the adhesion is weak, this geometry leads to a debonding by crack propagation without much fibrillation, even for a very soft layer.

EXPERIMENTAL SECTION

Materials and Sample Preparation

The adhesive used was an acrylic commercial pressure-sensitive adhesive, provided by Rhodia (Aubervillers, France), that was polymerized by emulsion polymerization. The main component of its monomer composition was 2-Ethyl-hexyl acrylate, and the glass transition of the PSA was measured at -55°C by differential scanning calorimetry. The samples were prepared from a 55% solids content emulsion in water. An excess amount of latex was deposited on a standard microscope glass slide and doctor bladed in order to obtain a final thickness of 100 μm in the dry film. The wet layer was slowly dried at room temperature for 24 h followed by 8 h in a vacuum chamber at

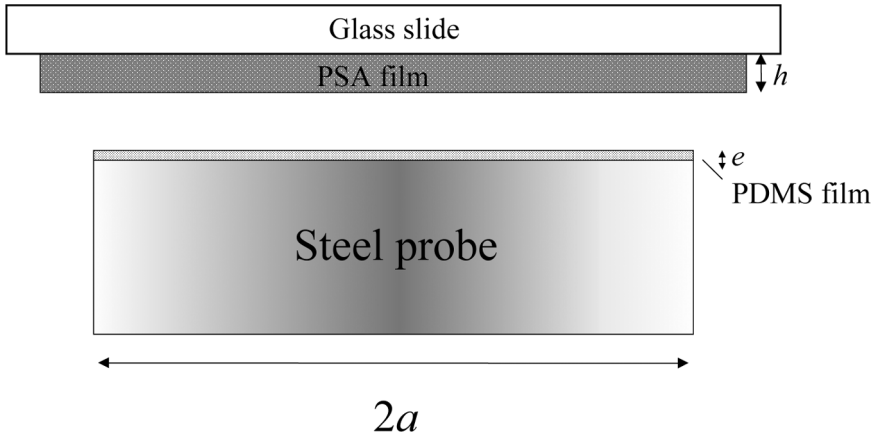

FIGURE 1 Confined geometry schematic with main geometric parameters.

45°C. This procedure was designed to ensure a dry sample but not to require special precautions to remove completely any trace of water, since the adhesion test was not performed in a humidity-controlled chamber. However, it should be noted that the humidity of the room was never very far from 50%, so we feel that our results should not be affected by variations in the moisture content of the air.

The flat surface of the cylindrical probe was coated with a 1 μm thick layer of a three-component, curable, commercial silicone elastomer which was provided by Rhodia. The specific silicone formulation was chosen as a model low adhesion material for the purpose of developing the method. It was a simple crosslinked PDMS elastomer with no additional additive but with a distribution of molecular weight of the chains between crosslinks. The material chosen was almost perfectly elastic with an elastic modulus $E' = 0.8$ Mpa, frequently independent at room temperature.

After deposition of the three-component solution by spin-coating, the probe was cured at 150°C for 4 h. The stoichiometry of the components was chosen in order to obtain an optimum degree of crosslinking. The resulting layer thickness was around 1 μm and very homogeneous across the surface. It should be noted, however, that the long wavelength roughness of the metal surface could not be avoided and was not corrected by the PDMS layer. It should also be pointed out that the remaining soluble fraction (2–3 wt%) of PDMS in the crosslinked layer was not extracted after curing. This procedure was chosen to work with a material as close as possible to the situation encountered in practice.

Experimental Apparatus

The accurate measurement of the deformation of a highly confined layer poses some specific experimental problems because of the great variation in the compliance of the layer during a test, and generally because of its low value relative to the compliance of the apparatus itself. Ideally one would like to perform mechanical tests either in force control (with an apparatus much more compliant than the sample) or in displacement control (with an apparatus much less compliant than the sample) However, during the course of a tensile test of a soft confined layer, the compliance of the layer can increase by two orders of magnitude during the test, as discussed in the Appendix. Therefore, it is nearly impossible to design a testing machine which has both the sensitivity necessary to measure the force in the high compliance region of the test and the stiffness required to perform a displacement-controlled test in the low-compliance regime. Additionally, the large increase in the compliance of the soft adhesive layer is known to be due to the formation of cavities or cracks within the layer that reduce significantly the degree of confinement. In order to interpret properly the force versus distance curves obtained from the test, it is very useful to be able to visualize the failure process in real time.

The mechanical and visualization requirements motivated us to develop a new instrument specifically optimized for the mechanical testing of soft confined layers. From the design point of view we have chosen a technical solution which is a compromise. The sensitivity has been favored, and the compliance of the apparatus and sample holder are measured as precisely as possible.

The design of the testing apparatus is as shown in Figure 2. Mechanically, three stepping motors are driving the upper plate at the same velocity while a central motor is driving the flat-ended probe. The adhesive layer is deposited on a glass microscope slide using a procedure that is described in the materials section. The slide is then fixed on the upper plate with the adhesive layer facing downwards. The load cell is placed in series with the probe, while an optical sensor is positioned between the plate and the probe in order to measure as accurately as possible the distance between the substrate and the probe.

The choice of a tripod and a single motor for the drive is motivated by three experimental aspects:

- the need to align as precisely as possible the surface of the adhesive layer relative to the probe surface,
- the need to free as much space as possible for the optical observation of the test with a microscope, and

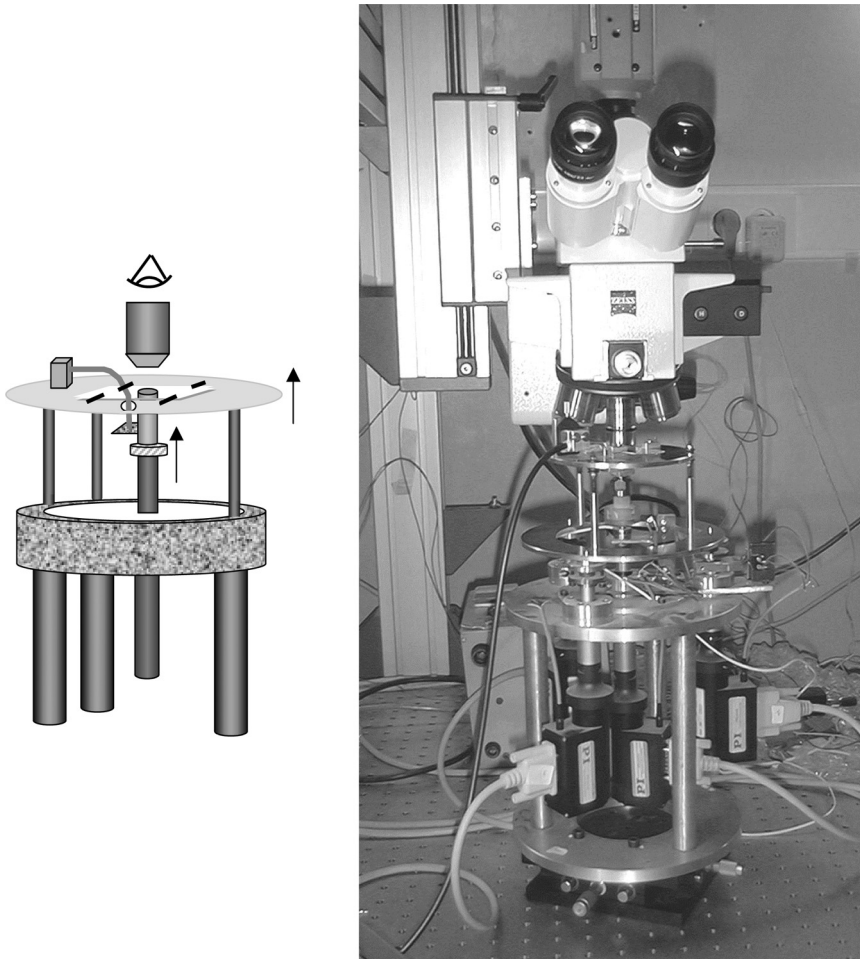

FIGURE 2 Schematic of the microtack tester with microscope viewing capability.

- the need to avoid the mechanical slack when a motor changes direction.

The specific alignment problem implies the ability to adjust, with some precision, the sample orientation in order to be as parallel as possible to the surface of the probe. In practice, this is done with three adjustable screws on the three legs of the tripod. Once the alignment is good (as checked by optical fringes), the screws are tightened and the

apparatus can be used for a test. If the surface of the adhesive layer is flat and the probe has been suitably righted and its surface polished, the contact takes place on the entire probe and a confinement ratio (defined as the ratio between the probe radius and the layer thickness) as high as 60 can be achieved. In the tests described in this article the probe radius was 3 mm and the layer thickness 100 μm, giving a degree of confinement of 30.

The observation of the microscopic mechanisms taking place during the debonding process requires an observation point where the interface between the probe and the film can be visualized. In our apparatus, the sample holder being upside down, the space is free above the sample. If the sample holder is transparent, the only requirement is that of a working distance of the lens of at least 2 mm. This is easily achievable, and we have fitted a series of long-working distance lenses, ranging form 1.5X to 50X to a Zeiss microscope head. This gives a full screen field (width) of view ranging from 9.6 mm to 240 μm. It is worthwhile to note that using a microscope rather than a standard zoom lens on a CCD camera has the distinct advantage of giving a better contrast in the images thanks to its epi-illumination, and it also allows the use of other optical techniques (such as fluorescence [21]). This is particularly useful for the automated digitization of the black and white images of the debonded and not-debonded areas of the surface of the probe. The microscope is then fitted with a CCD camera, and the images during the test are fed to a VCR but can also be directly captured by a computer.

Finally, in order to solve the third aspect, the test is performed schematically in the same way as in Figure 3, *i.e.*, the probe moves in contact with the sample and then the upper plate is removed from the probe. In this way all motors move in the same direction and no mechanical slack in the motors is observed when changing the direction of loading. The displacement sensor is shown schematically in Figure 2. It is an optical sensor (Philtec D63 LPT, Philtec, Annapolis, MD, USA) which, once properly calibrated, measures the distance between the upper plate and the probe with a precision of 0.4 μm but a relative resolution closer to 0.2 μm and a maximum range of 700 μm in the large linear range. The distance measurement includes the deflection of the glass slide over which the sample is deposited. Suitable calibration tests on a slide without an adhesive layer provide us with the deflection of the bare slide as a function of the applied force. This displacement sensor is essential in the first stages of the test, where the compliance of the layer is smaller that that of the apparatus. When the displacement of the motor is above 500 μm and typically the detachment test is in its fibrillation stage, the displacement that

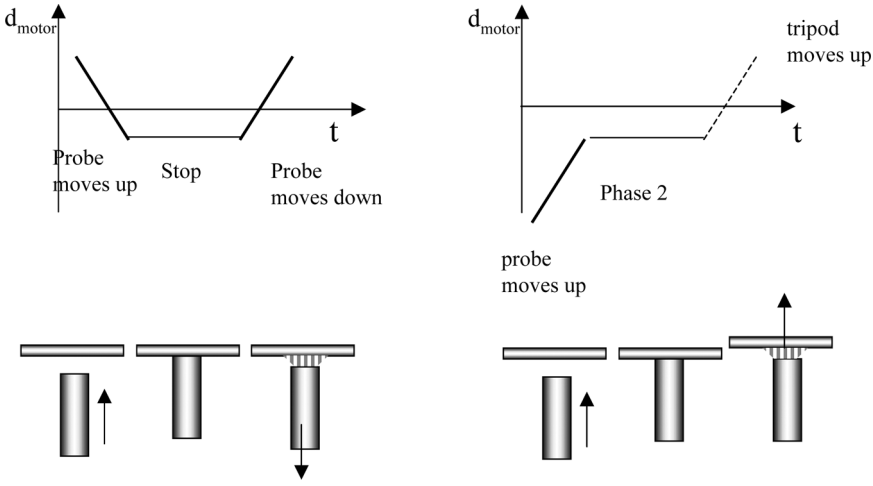

FIGURE 3 Schematic of the mechanical motions in a probe test. (a) Classical design: the probe is the only mobile part. (b) New design: both probe and sample holder move in the same direction, avoiding the mechanical slack involved with changing directions on the stepping motor.

the sample sees is identical to that of the motors. For the experiments described here the compliance of the apparatus is of 4.4 μm/N. Note that both the displacement resolution (0.2 μm) and force resolution (0.1 N) are much better than what was obtained with the previous probe tester [22] while maintaining the possibility to go to large displacements (up to 25 mm) and to test highly confined layers (up to $a/h = 65$) with a good enough alignment between probe and film.

Finally, in terms of computer control and data acquisition, the stepping motors (PI Instruments Karlsruhe, Germany) and the separate acquisition card (Data Translation DT301, Malboro, USA) are controlled by a National Instruments Labview software module (National Instruments, Austin, TX, USA) developed by the authors. The experimental data obtained from a test are the force, displacement of the motors, and sensor displacement as a function of time. In addition, at the beginning of each test the computer sends a signal to an outside timer which prints the time on the image recorded on the VCR therefore, synchronizing, the time on the force-displacement data file and the time on the video captures of the test taken by the CCD camera shown in Figure 2.

The debonding experiments of the confined layer were performed as follows: The probe is brought in contact with the layer at a constant

motor velocity of 10 μm/s. Once the probe touches the adhesive layer, the layer and the apparatus start to deform. When a compressive force of 5 N is attained (corresponding to an average compressive stress of 0.2 MPa if the probe if fully in contact), the probe motor is stopped. After 1 s the motors driving the upper plate are set in motion at a constant retraction velocity of 10 μm/s.

Two different types of tests were performed:

- nonstop tests where the motors are driven until full detachment of the adhesive from the probe occurs.
- stop tests, where the upper plate motors are stopped once the force reaches a preselected positive value (in tension with our sign convention). At this point, with all motors idle, the force and displacement are recorded as a function of time. A certain amount of elastic energy is stored during the loading part of the test and can be released during this stage.

Additional information can be gathered from the video images. The stored elastic energy can be released in three ways: by a viscoelastic relaxation of the adhesive (a bulk dissipation process), by the nucleation and subsequent growth of cavities in the bulk or at the interface, or by the propagation of interfacial cracks (an interfacial dissipation process). In order to examine these possible scenarios, we have measured the debonded area as a function of time by using the digitized microscope images and therefore obtained both the nominal stress, σ_{nom}, defined as F/A_0, where A_0 is the area of contact at the time of maximum compression, and σ_{true}, defined as F/A, where A is obtained by measuring the area still in contact with the probe. Clearly, in such a configuration the true stress in the layer is highly inhomogeneous. However, we feel that this approximate definition can be useful in capturing the physics of the process of detachment of the adhesive layer from the surface of the probe.

Viscoelastic Properties of the Confined Layer

In order to interpret our adhesion data properly, it was essential to perform a rheological characterization of our adhesive. This was done on a Rheometrics RDA II parallel plate rheometer (Rheometrics, Austin, TX, USA). A 2 mm thick sample of adhesive was prepared by slow evaporation of the water and placed between the parallel plates of the rheometer.

Two types of characterization were performed. A classical linear viscoelastic characterization in oscillatory shear was performed as a

function of frequency at temperatures varying between $-30^{\circ}C$ and $70^{\circ}C$. From these data, a master curve of G' and G'' was constructed using the time-temperature superposition principle and is shown in Figure 4a. Clearly the adhesive behaves as a lightly crosslinked polymer gel, exhibiting a strong frequency dependence of both the elastic and viscous part of the modulus. It is interesting to note, however, that at low frequencies G' is nearly constant while G'' keeps decreasing, indicating a material which becomes increasingly elastic at low frequencies. In order to simulate the relaxation process occurring during stop tests, a relaxation test has also been performed in the rheometer. In this case a step strain is imposed and the rheometer is maintained at a fixed value of torsion angle, and the moment is monitored as a function of time. This measurement provides the relaxation modulus as a function of time G(t). Note that the relaxation modulus is nearly independent of the amplitude of the initial deformation applied to the layer as shown in Figure 4b. This is indicative of a linear viscoelastic behavior up to very large strains.

RESULTS

The force versus time curves of two nonstop tests performed at a drive velocity of 10 μm/s (on steel and on the PDMS surface) are shown in Figure 5 with their corresponding images. When a tensile load is applied, the layer is initially strained more or less uniformly. Around the maximum force the interface fails either by the nucleation and propagation of internal cracks (on steel) or by the propagation of finger-like edge cracks (on PDMS). In both cases the steep decrease in force is due to the propagation of the cracks. It is, however, immediately apparent from the comparison between the two curves that, while maximum measured nominal stress is nearly identical for both surfaces, the velocity at which these cracks propagate is very different, much slower on the steel surface than on the PDMS. This result indicates that crack initiation may be insensitive to the nature of the probe surface but crack propagation is certainly not.

A second important observation should now be described. In Figure 6, four force-displacement curves are shown where the probe is removed at different velocities ranging from 1 to 100 μm/s. Clearly, the viscoelastic behavior of the adhesive comes into play at and after the maximum stress, but the initial slope of the force-displacement curve is unaffected within our experimental resolution. The interpretation of this result is that we are deforming the adhesive nearly elastically until failure starts, at which point dissipative processes related to the formation and growth of interfacial cracks occur. We

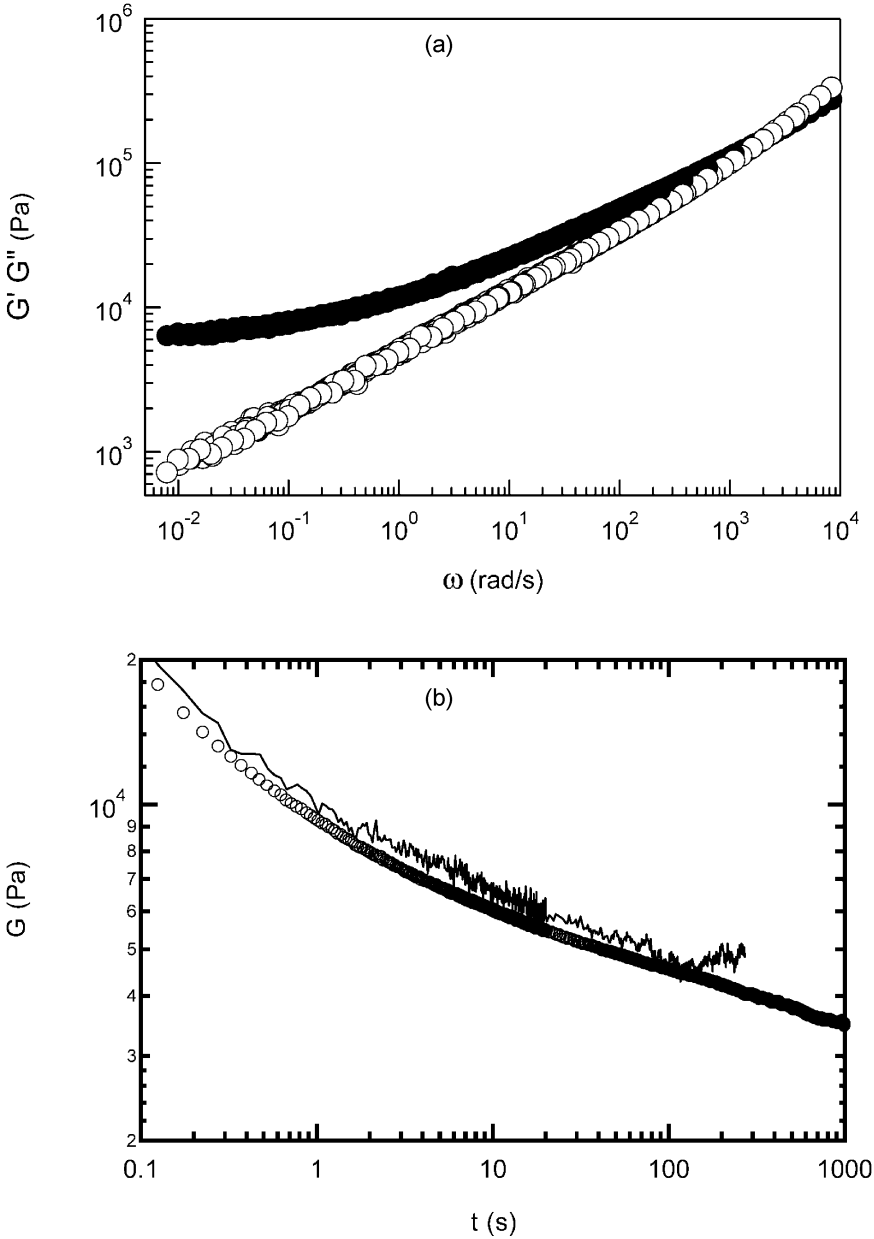

FIGURE 4 (a) G′(●) and G″(○) as a function of reduced frequency $a_T\omega$. (b) Relaxation modulus G(t) for the adhesive as measured in a parallel plate rheometer: (○), initial strain 80%; full line, initial strain 5%.

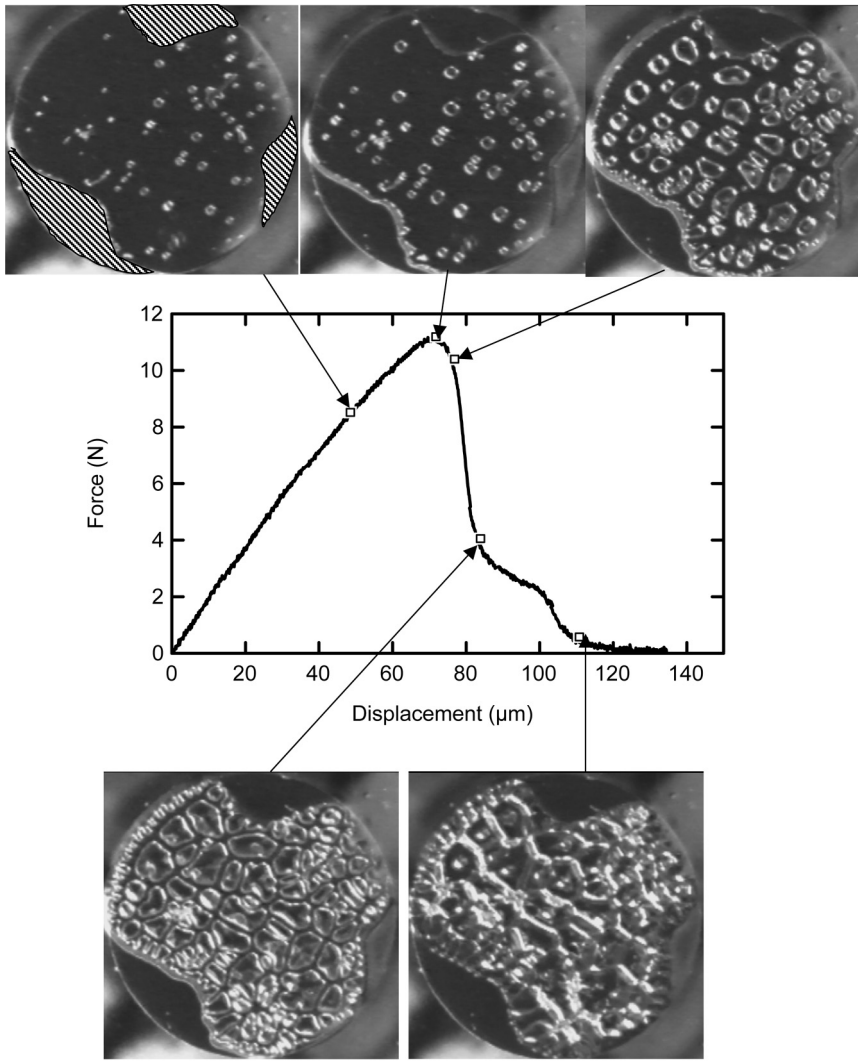

(a)

FIGURE 5 Force *versus* time curves of the same adhesive detached from (a) a steel surface and (b) a PDMS surface. The images have been synchronized with the force–time curves and show the progress of the debonding. The experiment in 5(a) has been performed at a debonding velocity of 100 μm/s, while the experiment in 5(b) has been performed at 10 μm/s. The contact time was 1 s and the contact pressure 1 Mpa for both experiments. In both figures, the shaded area shows the part of the probe that was never in contact with the adhesive because of misalignment. (*Continued.*)

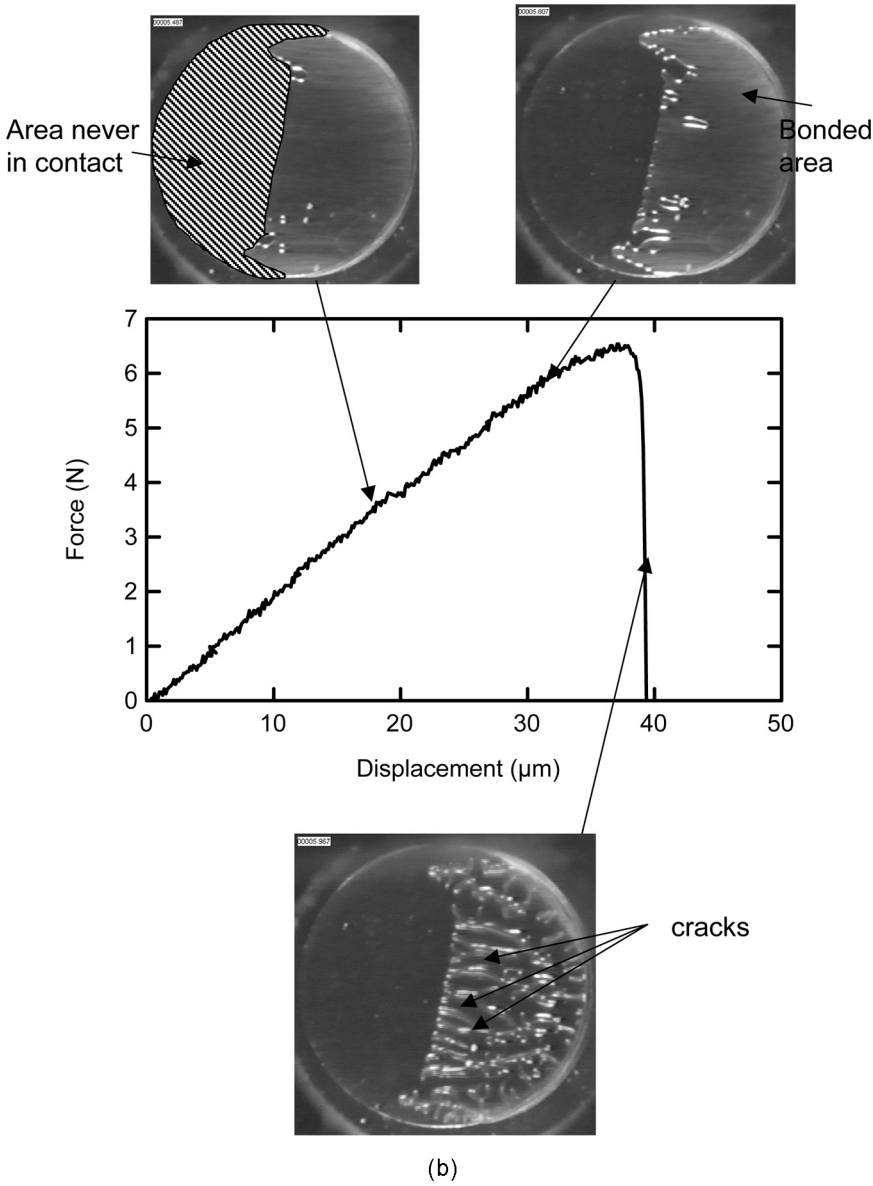

FIGURE 5 (Continued.)

believe that this nearly elastic stretching of the adhesive is due to the high degree of confinement and the relatively low compliance of the layer relative to the apparatus which strongly limits the deformation

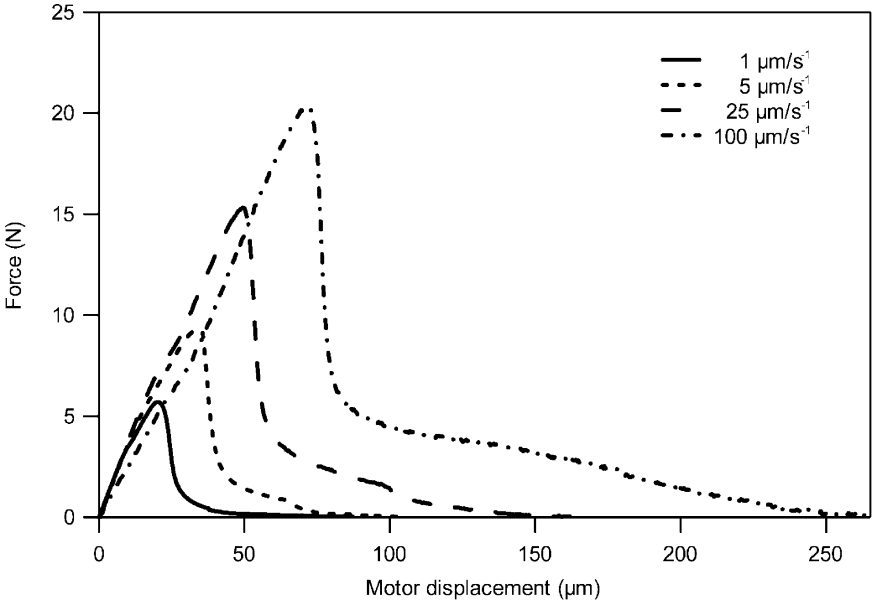

FIGURE 6 Force-displacement curves of probe tests of the PEHA adhesive on a steel surface at different probe retraction velocities. Contact times and contact pressure are identical for all experiments.

of the layer. Furthermore, optical observations show that the edge of the contact undergoes large strains locally that undoubtedly modify the compliance of the layer relative to what can be calculated with an infinitesimal strain theory [8, 23].

Based on these two observations, a better quantification of the effect of adhesion on crack velocity can be obtained with the help of the stop tests described in the experimental section. The force *versus* displacement curves and force *versus* time curves of a series of tests where the probe was stopped at increasing values of tensile force are shown in Figure 7 for the PDMS surface. As one can see, the later the stop the faster the relaxation of the force. Effectively one measures how fast a certain amount of elastic energy (the area under the force displacement curve) can be dissipated. Since no other external work is put in the system, and nearly all the energy under the force-displacement curve is elastic, this method of calculating the initial stored energy is a very good approximation.

It should be noted that the compliance of the apparatus plays a role here. As discussed in more detail in the Appendix, part of the energy is

stored in the apparatus. The more compliant the apparatus, the greater the amount of stored energy. This has two interesting consequences: The softer the apparatus the faster the detachment occurs (since the elastic energy release rate is limited by the dissipation occurring during crack propagation which is apparatus independent) and the less error one makes on the calculation of the integral under the triangle ABC in Figure 8. Then the elastic energy stored is directly

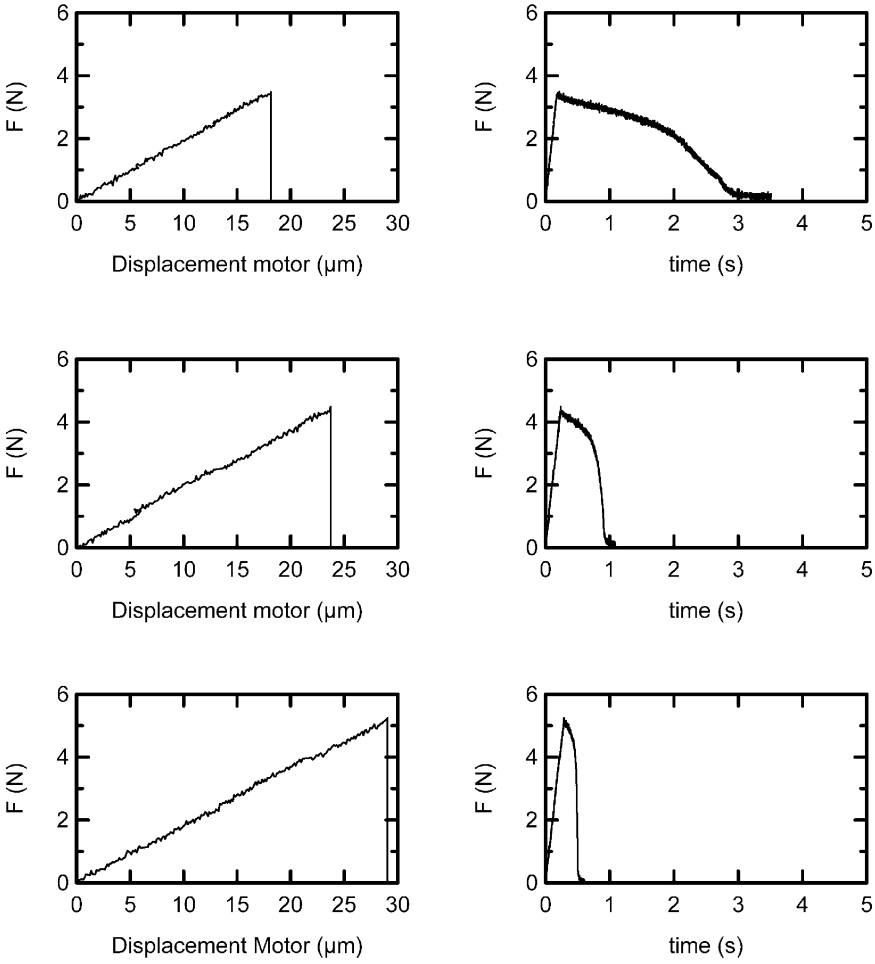

FIGURE 7 Measured force as a function of displacement (left) and as a function of time (right) for three probe tests where the motor has been stopped progressively later in time.

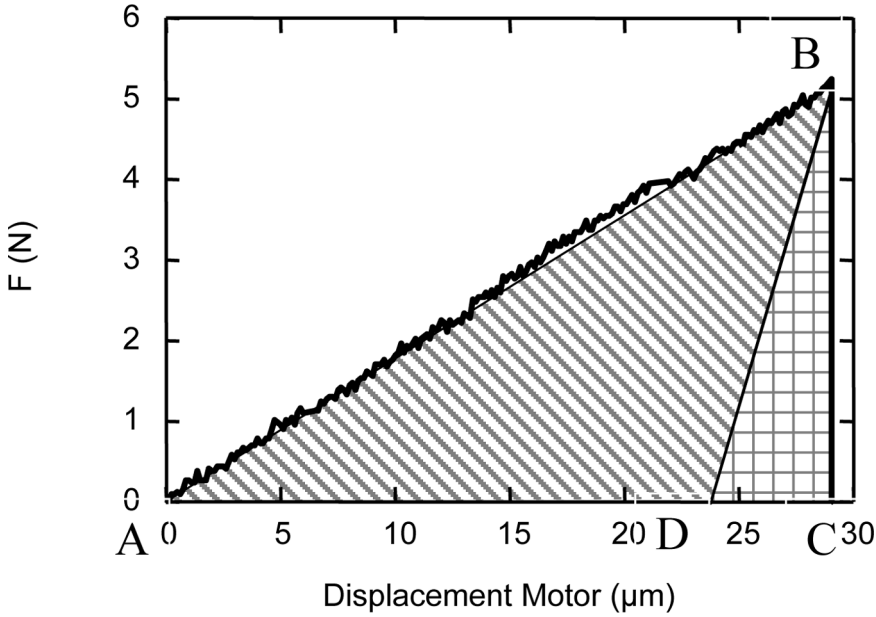

FIGURE 8 Force-displacement curve showing schematically the effect of the compliance and the fraction of elastic stored energy in the layer and in the apparatus. The shaded area delimited by points A, B, and D represents the elastic energy stored in the apparatus, while the area shaded with small squares delimited by points B, C, and D represents the energy stored in the layer. Both energies are released during detachment of the adhesive from the surface.

controlled by the displacement of the motors. With a soft machine, a small change in stored energy corresponds to a significant displacement of the motors and so one can control fairly precisely the amount of elastic energy which is stored in the system before relaxation starts. The second question however, is, how is this energy dissipated from point B to point C? Figure 7 shows that the rate at which the elastic energy is dissipated is clearly quite different depending on where the stop occurs. This result is not very consistent with a relaxation of the force by the viscoelastic relaxation of the adhesive. In fact, this argument would predict a relaxation occurring in a nearly identical way regardless of the extent of deformation (see Figure 4b).

The analysis of the video images shows, however, that for all three stop tests of Figure 7, the relaxation of the force occurs by the propagation of multiple cracks at the interface between the probe and the adhesive film, as shown in Figure 9. As a result, the true contact area

between the probe and the film decreases dramatically during this decrease in force.

This can be made into a more quantitative measurement by assuming that only the bonded area can sustain stress. Figure 10 shows the nominal and true average stress on the layer as well as the debonded area as a function of time during the relaxation. Apparently, at least in the initial part of the relaxation process, most of the relaxation of the force can be attributed to the reduction in load-bearing area caused by the propagation of cracks at the interface between the probe and the film. Therefore, one would be tempted to conclude that since the true stress, defined as the force divided by the actual load-bearing area, remains nearly constant, the elastic energy stored in the layer is proportional to the load-bearing area. However, since the apparatus is compliant, a large relaxation of the force (from 3.9 N to 2.2 N in the example of Figure 10) implies a decrease in the deformation of the apparatus and, of course, an increase in the deformation of the adhesive layer (7.8 μm of additional displacement for the adhesive layer corresponding to an additional strain of 7.8%). Effectively, an external work is performed on the layer, and in reality a constant true stress means an increase in the effective compliance of the polymer being stretched. This increase could be due to the significant reduction in confinement, which has been shown to increase the compliance of fully elastic layers, but also to the creep of the polymer itself through its compliance function J(t). At this stage it is difficult to separate the two effects. However, if the experiment is carried out until the layer completely detaches from the surface, the total energy dissipated normalized by the area of the probe has the meaning of an average adhesion energy per unit area which we will define as $\langle \mathcal{G}_c \rangle$.

The way forward is then to define an average crack propagation rate for each experiment. A very simple but reasonable approximation is to define a crack velocity as the radius of the probe divided by the time elapsed between the stop and the relaxation of the force to zero, which is indicative of the final detachment. Of course, both the rate at which energy is released and the crack velocity are not constant during the detachment process. Furthermore, the crack propagation rate is spatially inhomogeneous and the shape of the crack resembles more that of fingers than that of a simple annular crack. This is shown in Figure 9 for a series of stops at different force values for the PDMS surface. However, a detailed analysis of the propagation process would be much more complicated without adding much to the general picture here. In fact, since these tests were performed with the same probe, the shape and position of the fingering cracks in Figure 10 are nearly identical from one experiment to another. This means that the

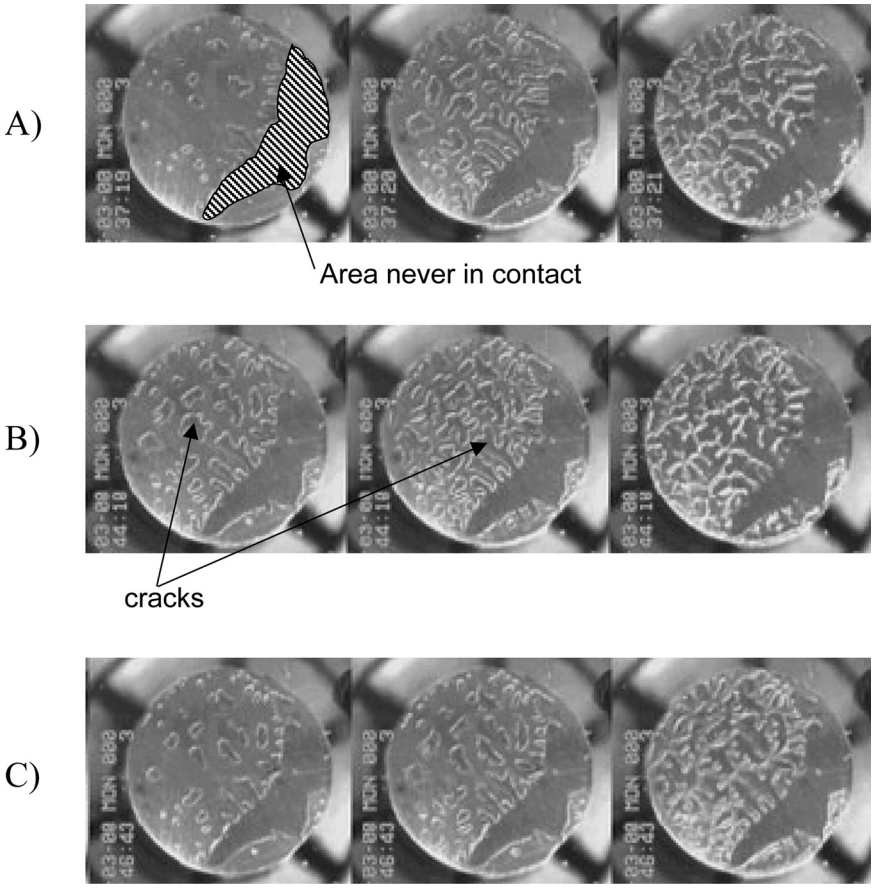

FIGURE 9 Images of debonding for the tests shown in Figure 7: (a) $F_{stop} = 3.4\,N$; (b) $F_{stop} = 4.3\,N$; (c) $F_{stop} = 5.2\,N$. In the upper left image, the shaded area shows the part of the probe which was never in contact with the adhesive because of misalignment. Since the probe remains the same for the three tests illustrated here, this area also remains the same.

distribution of crack propagation rates remains the same for all experiments performed with the same probe, and only the *average* crack velocity changes.

With these approximations, the energy released during the relaxation of the force, and the average velocity of the cracks which propagate during this release $\langle v \rangle$, can be computed for each stop. If the energy released is then divided by the surface area which is being debonded, the equivalent of the more familiar $\langle \mathcal{G}_c \rangle$ *versus* $\langle v \rangle$ curve

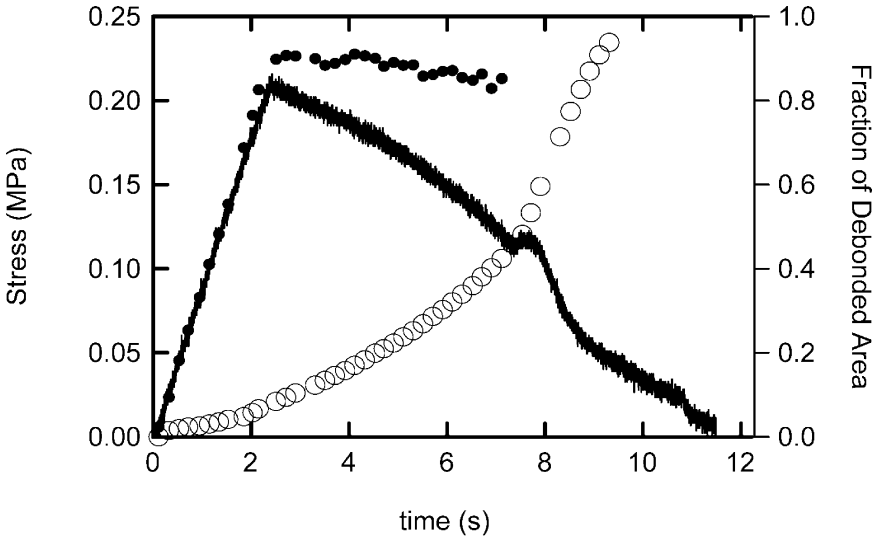

FIGURE 10 Nominal (full line) and true (●) stress as a function of time during a relaxation experiment. The adhesive is detached here from a steel surface, and the fraction of contact area which is detached as a function of time during the relaxation process is shown on the righthand scale (○). The duration of the stop is 5 s, after which the motors are restarted and the adhesive detaches.

associating an energy release rate with a crack velocity [6, 8], can be obtained. Increasing the displacement of the motor before the relaxation begins leads to an increase in the initially stored elastic energy and, as a result, to higher crack velocities when the layer is detached. Then part of the $\langle \mathcal{G}_c \rangle$ *versus* $\langle v \rangle$ curve can be measured. An alternative way to analyze the data would be to measure $\langle \mathcal{G}_c \rangle$ *versus* a debonding time which becomes shorter as the initially stored elastic energy increases.

Two such curves (for the steel and for the PDMS surfaces) are shown in Figure 11. Interestingly, the absolute values of $\langle \mathcal{G}_c \rangle$ which are measured (at low rates of propagation) are very close to what is measured in a JKR test between a typical acrylic adhesive and the same PDMS surface [2]. However, the range of crack velocities experimentally accessible is different from what can be conveniently achieved in a JKR test spanning the μm/s range rather than the nm/s. Since the calculation of the total dissipated energy is exact, this result implies that the detachment of a soft adhesive from a silicone layer at crack front velocities of the order of a few microns/s requires very little deformation of the polymer in the bulk.

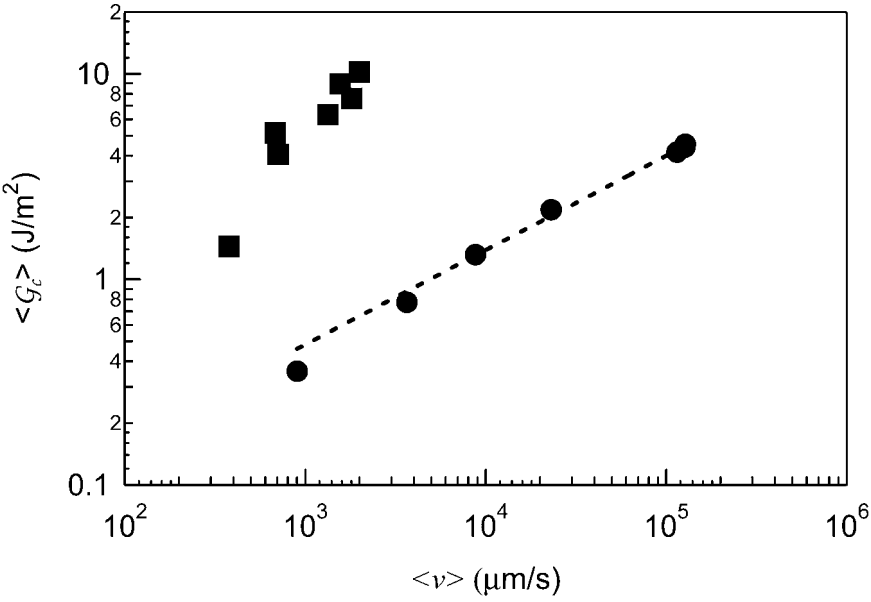

FIGURE 11 $\langle \mathcal{G}_c \rangle$ *versus* $\langle v \rangle$ curves for the same adhesive on two surfaces, steel (■) and PDMS (●).

The $\mathcal{G}_c$ *versus* v data can then be fitted with an expression used for JKR tests for the adhesion of crosslinked elastomers on a solid surfaces [8], *i.e*,

$$\langle \mathcal{G}_c \rangle = \mathcal{G}_0 \left(1 + \left(\frac{\langle v \rangle}{v^*} \right)^n \right), \tag{1}$$

where $\mathcal{G}_0, v^*$, and n are adjustable parameter. The adhesion of well-crosslinked elastomers on a solid substrate n is typically around 0.5–0.6 [6, 8], while $\mathcal{G}_0$ is on the order of the thermodynamic work of adhesion, and v^* depends on the experimental geometry but has a physical meaning of sensitivity to the debonding rate. For a given geometry, the lower v^* is the more dissipative is the crack propagation process.

Since the data can be fitted with many combinations of parameters, in order to get sensible values one needs to fix at least one of them. For the PDMS surface we fixed $\mathcal{G}_0$ at 45 mJ/m^2 as measured from similar experiments done with JKR tests by Amouroux *et al*. [24]. In this case, the best fit to the data gives $v^* = 7.3\,\mu$m/s and $n = 0.47$.

For the steel surface, it is more difficult to fix $\mathcal{G}_0$ since there is no direct way to detach such an adhesive from a steel surface with a vanishing amount of dissipation (the adhesive would deform for such a viscoelastic adhesive). However, based on results obtained by Crosby and Shull [25], the results for this particular type of adhesive on steel are reasonable quantitatively. If we fit the data with a powerlaw, the exponent, n, that best fits the data is $n = 1$. Interestingly, this value implies a much more dissipative crack propagation process than in crosslinked elastomers, in agreement with the highly viscoelastic nature of the adhesive.

DISCUSSION

Our results show that, at least for certain types of viscoelastic adhesives and surfaces, it is possible to define an amount of dissipated energy related to the propagation of interfacial cracks. Therefore, if one defines adhesion as the ability to dissipate energy upon separation of the two surfaces, our method provides a way to quantify and compare the adhesion of different adhesives on the same surface or the same adhesive on different surfaces without incorporating any dissipation due to large strains or fibrils.

Since this article focuses on methodology, it is worthwhile at this stage to discuss critically the comparison between the flat-probe method and competing methods designed to quantify adhesion between a solid substrate and a soft viscoelastic layer. The most common methods are the peel test and the so-called JKR test, where a spherical indenter is brought in contact and subsequently removed from the adhesive surface. The peel test has been used for a long time as the industry standard for adhesion tests due to its simple setup and good reproducibility. Relative to the flat probe test, the peel requires much less precision mechanically, allows very long contact times, and is essentially a crack propagation test. The disadvantage of the peel test, however, is that the level of strain attained by the adhesive layer before detachment is not limited by the geometry and can extend well into the fibrillar regime. Therefore in practice it is difficult to distinguish between a high peel force due to fibrillar formation and a high peel force due to an interfacial dissipative crack propagation. In other words, the peel test gives the equivalent of the integral under a force-displacement curve of the probe test and cannot distinguish between a high force and small displacement and a low force and large displacement. The probe test applies, on the contrary, a given energy release rate at a fixed displacement (which can remain low) and measures crack growth rate. When, for a given applied energy release rate,

the crack growth rate vanishes, fibrillar growth becomes the only possible deformation mechanism and is clearly no longer related to the adhesion at the interface. In this regime, adhesion is "sufficient" and the practical work of detachment is only dependent on the rheological properties of the adhesive layer.

Nevertheless, in the case where adhesion is weak (as for the adhesion on a PDMS elastomer), fibrillar structures are not observed and the peel test should give very similar results to the probe test. Indeed, the peel test results obtained by Amouroux *et al.* [2] on the same surface but with another adhesive give similar low values of the adhesion energy and a similar rate dependence.

In this system, the low values of adhesion energy for the peel tests have been attributed to an interfacial slippage precluding much shear deformation in the adhesive layer. A similar argument can be applied to the confined layer. At the edge of the layer very large interfacial shear stresses are applied by a macroscopic tensile force on the probe due to the confinement. It is possible that interfacial slippage greatly reduces these shear stresses and facilitates the growth of an interfacial crack.

The other technique that has recently been extended to viscoelastic materials is the spherical probe test. It should be stressed that if the adhesive is viscoelastic but not able to form a fibrillar structure the bonding and debonding of the indenter from the adhesive can be quantitatively analyzed with the tools of viscoelastic contact mechanics. However, in practice, the difficulty is that the bulk and interface dissipation cannot be separated, neither during the loading nor during the unloading process. This does not give rise to a well-defined value of $\mathcal{G}_c$ (The modulus E varies continuously during the loading and precludes a reasonable or even approximate calculation of the stored elastic energy), but only to a well-defined value of the stress intensity factor, K_1, at the crack tip. One can, therefore, obtain a curve of K_c *versus*, v, which in principle can be compared between systems but which is not easily converted to a level of dissipated energy.

In our flat probe method, on the other hand, the loading part (see Figure 6) is essentially elastic and can be readily evaluated even for fairly viscoelastic materials such as the model adhesive used in this study. Then this elastic energy is dissipated during the multiple crack propagation process. The released elastic energy (in the layer and in the apparatus) is, of course, not uniquely dissipated at the interfacial plane but in a volume limited by the applied macroscopic displacement and which excludes fibrils (typically about 20–30% deformation for our 100 μm thick films as shown in Figure 7). As long as the relaxation of the force occurs by the lateral growth of cavities it is a measure of

the adhesion at the interface. We believe, therefore, that the method has some potential usefulness, in particular to compare quantitatively the interfacial adhesion as opposed to the ability to form the fibrils and the dissipation during fibrillar growth.

Despite the advantages which were pointed out above, it is also important to point out the limitations and inherent approximations made in the evaluation of $\langle \mathcal{G}_c \rangle$:

- In reality, a probe test is performed by indenting the viscoelastic layer with a flat-ended probe until a given compressive force is attained. At that stage, the probe is removed from the layer at a constant velocity. Therefore, one should in principle consider the whole deformation history of the layer to simulate its behavior in tension. However, as an approximation we have neglected here the compressive part of the test and focused on the tensile part as if the test had begun as a tensile test at $F = 0$ with the probe fully in contact with the layer. Our own experiments have shown that if a sufficient constant compressive pressure is applied on the layer and the storage modulus of the layer G' at 1 Hz is below about 0.1 MPa, the compression stage has little effect on the tension results. However, as a precaution, the conditions of the compression stage should be kept constant when testing a series of adhesives on the same surface or the same adhesive on a series of surfaces.
- While the procedure of stopping the test and letting the system relax is widely applicable, the result is not necessarily crack propagation but could be simply the nucleation of new cracks or cavities or the viscoelastic relaxation of the adhesive in the layer without any fracture event. Clearly, the interpretation of the dissipated energy as being an adhesion energy depends on the existence of propagating interfacial cracks during the relaxation process. This fact needs to be checked with an observation method.
- In a fracture test the value of G_c does not depend on the thickness of the layer since dissipation should be confined very near the interface. This was not checked in our system and while the propagating of the cracks is clearly at the interface, it is not obvious that the measured $\langle \mathcal{G}_c \rangle$ does not depend on the initial layer thickness. Therefore, for comparative purposes it is better to keep the adhesive layer thickness constant.

Coupling Between Compliance and Adhesion

It is important at this stage to discuss the important role played in this experiment by the compliance of the apparatus. If the separation

between the adhesive and the surface were reversible and independent of the rate at which it occurs, the compliance of the apparatus would not play a role. However, Barquins and Maugis have shown that for a crosslinked elastomer on a solid surface there is a unique relationship between the elastic energy release rate, $\mathcal{G}$, and the velocity at which a crack propagates, and a version of this relationship is given in Equation (1). In essence, this reflects the fact that the dissipation at the crack tip is dependent on the crack velocity. As we can see from Figure 11, we find in our experiments a very significant dependence of the adhesion energy on the average crack velocity.

In the above section "Materials and Sample Preparation," we have seen that when a tensile force is applied to the layer, the energy release rate increases. As soon as $\mathcal{G}$ increases above $\mathcal{G}_0$ the crack starts to move and the compliance of the layer decreases. When the compliance of the layer becomes of the order of the compliance of the apparatus the crack accelerates rapidly, the force drops, and the layer sees a very rapid increase in the plate separation, h, which enhances the acceleration of the crack. The apparatus acts in effect as an energy reservoir which is then suddenly emptied when fracture occurs. An identical effect, although due to different mechanisms, is observed for fluid adhesion [26, 27].

Therefore, a change in the compliance of the apparatus will change the size of the reservoir for a given applied tensile force. The more compliant the apparatus, the less error is made in measuring the stored elastic energy in the loading stage and the larger the energy reservoir. Therefore, when the cracks propagate, the measured crack velocity will be higher for the more compliant apparatus since, for the same decrease in confinement and therefore in force, the rate of release of elastic energy increases. A more detailed discussion of the effect of the compliance on crack propagation is in the appendix.

CONCLUSION

We have shown that the adhesion between a soft layer and a hard surface can be measured by testing the layer in a confined geometry with a relatively compliant apparatus.

This geometry has two distinct advantages over the more classical spherical contact, mechanics geometry or the peel geometry:

- The loading and unloading are clearly separated stages, and the loading is confined and elastic while the unloading is viscoelastic. In a spherical indenter test these two stages cannot really be separated. During the loading stage, most of the energy is stored in

the apparatus, and if the loading is interrupted at a given force level the energy release rate can be effectively controlled. This energy is then dissipated by the propagation of several interfacial cracks at a given velocity which is dependent on the amount of stored elastic energy at the beginning of the stop. One effectively obtains a $\langle \mathcal{G}_c \rangle$ *versus* $\langle v \rangle$ curve measuring the amount of energy necessary for the crack to propagate at the interface at a given average velocity.

- Since the layer remains confined during the entire process of separation, the $\langle \mathcal{G}_c \rangle$ *versus* $\langle v \rangle$ curve that is obtained is representative of the interfacial dissipation and does not include any energy dissipated by fibril formation and growth (large strains). Again, in classical tests the opening displacement of the crack tip cannot be controlled and allows for crack blunting and fibril formation as discussed in a recent paper by Hui and Jagota [28].

Finally, it is quite clear that our work is rather exploratory and leaves the reader with many unanswered questions, but given the difficulty of the task we feel that the method is promising and deserves further investigation.

REFERENCES

[1] Léger, L., Hervet, H., Massey, G. and Durliat, E., *J. Phys: Cond. Mat.* **9**, 7719–7740 (1997).
[2] Amouroux, N., Petit, J., and Léger, L., *Langmuir* **17**, 6510–6517 (2001).
[3] Johnson, K. L., Kendall, K., and Roberts, A. D., *Proc. Roy. Soc. London*, *A* **A324**, 301–313 (1971).
[4] Hui, C. Y., Lin, Y. Y., Baney, J. M., and Jagota, A., *J. Adhesion Sci. Tech.* **14**, 1297–1319 (2000).
[5] Maugis, D., *Langmuir* **11**, 679–682 (1995).
[6] Maugis, D. and Barquins, M., *J. Phys. D: Appl. Phys.* **11**, 1989–2023 (1978).
[7] Maugis, D., *Contact, Adhesion and Rupture of Elastic Solids*, (Springer-Verlag, Berlin Heidelberg New York, 1999).
[8] Shull, K. R., Ahn, D., Chen, W. L., Mowery, C. L., and Crosby, A. J., *Macromol. Chem. Phys.* **199**, 489–511 (1998).
[9] Unertl, W. N., *J. Adhesion* **74**, 195–226 (2000).
[10] Shull, K. R., *Materials Science and Engineering R*, *Reports* **36**, 1–45 (2002).
[11] Creton, C. and Fabre, P., 2002, In: *Adhesion Science and Engineering Vol* I; *The Mechanics of Adhesion*, (Elsevier, Amsterdam, 2002), pp. 535–576.
[12] Creton, C., Hooker, J. C., and Shull, K. R., *Langmuir* **17**, 4948–4954 (2001).
[13] Williams, J. G., *Fracture Mechanics of Polymers*, (Ellis Horwood, London, 1987).
[14] Lin, Y.-Y. and Hui, C. Y., *J. Polym. Sci. B Polym. Phys.* **40**, 772–793 (2002).
[15] Baney, J. M., Hui, C.-H., and Cohen, C., *Langmuir* **17**, 681–687 (2001).
[16] Baney, J. M. and Hui, C. Y., *J. Appl. Phys.* **86**, 4232–4241 (1999).
[17] Lin, Y. Y., Hui, C. Y., and Baney, J. M., *J. Phys. D: Appl. Phys.* **32**, 2250–2260 (1999).
[18] Hui, C. Y., Baney, J. M., and Kramer, E. J., *Langmuir* **14**, 6570–6578 (1998).

[19] Haiat, G., Phan Huy, M. C., and Barthel, E., *J. Mech. Phys. Solids* **51**, 69–99 (2002).
[20] Barthel, E. and Haiat, G., *Langmuir* **18**, 9362–9370 (2002).
[21] Zhang Newby, B. M. and Chaudhury, M. K., *Langmuir* **13**, 1805–1809 (1997).
[22] Lakrout, H., Sergot, P., and Creton, C., *J. Adhesion* **69**, 307–359 (1999).
[23] Creton, C. and Lakrout, H., *J. Polym. Sci. B Polym. Phys.* **38**, 965–979 (2000).
[24] Amouroux, N., Ph. D. Thesis, Université Paris VI, Paris, France (1998).
[25] Crosby, A. J. and Shull, K. R., *J. Polym. Sci. B Polym. Phys.* **37**, 3455–3472 (1999).
[26] Francis, B. A. and Horn, R. G., *J. Appl. Phys.* **89**, 4167–4174 (2001).
[27] Derks, D., Lindner, A., Creton, C., and Bonn, D., *J. Appl. Phys.*93, 1557–1566 (2002).
[28] Hui, C. Y., Jagota, A., Bennison, S. J., and Londono, J. D., *Proc. Roy. Soc. London*, *A* **403**, 1489–1516 (2003).
[29] Barquins, M. and Maugis, D., *J. Adhesion* **13**, 53–65 (1981).
[30] Tirumkudulu, M., Russell, W. B., and Huang, T. J., *Phys. Fluids* **15**, 1588–1605 (2003).

APPENDIX

Because of the confined geometry of the layer the compliance of the sample is low, and the compliance of the apparatus cannot generally be neglected. While this is hardly a novelty in materials testing, the issue of the role of the compliance of the apparatus on the results of the tests is rarely discussed within the context of probe tack tests of soft adhesives, and it is interesting to discuss its potential influence on the results and also how the apparatus can be optimized to the user's advantage. Barquins and Maugis have discussed the case of the detachment of a spherical indenter from a compliant apparatus [29], and we will extend their analysis to the case of the cylindrical indenter.

Compliance of a Thin Elastic Layer

The compliance of a thin elastic layer can be calculated by finite elements or by using an approximate analytical expression, if the two elastic constants of the material (typically the bulk modulus, K, and the shear modulus, G) are known. A convenient semiempirical expression spanning a wide range of degrees of confinement has been proposed by Shull *et al*. [8], and for the compliance of the layer it gives

$$C = \frac{3}{8Ea}\frac{\dfrac{0.75}{\alpha+\alpha^3}+\dfrac{2.8(1-2\nu)}{\alpha}}{1+\dfrac{0.75}{\alpha+\alpha^3}+\dfrac{2.8(1-2\nu)}{\alpha}}, \tag{A1}$$

where α is the ratio of the probe radius over the thickness of the layer a/h, ν is Poisson's ratio and E is Young's modulus.

Such an expression assumes infinitesimal strains and a no-slip boundary condition, which are not necessarily met in our experiments. It is, however, useful to obtain a first-order approximation of the compliance of the layer. If one assumes a shear modulus of the layer of 10^4 Pa and a bulk modulus, K, of 10^9 Pa, the expression in Equation (A1) gives a predicted compliance of 0.11 μm/N. Experimentally, typical measured values of the compliance for a 100 μm thick layer of soft adhesive are on the order of 1 μm/N, which remains significantly lower than the compliance of the apparatus, which is about 4.8 μm/N in our set of experiments.

However, qualitatively the change in compliance when the interfacial cracks propagate can be quite large, so that in practice the compliance of the apparatus is initially higher than that of the sample and becomes lower once significant crack propagation occurs.

The important consequence of this change in compliance in mid-test is that the deformation rate that the sample sees is not uniform throughout the test.

True Average Strain Rate of the Sample

If one considers only the debonding stage of a probe test in which the probe is nominally removed from the adhesive at a constant velocity, it can be divided roughly into three stages. In the first stage, the strain rate of the sample is constant but lower than the strain rate set by the drive. In the second stage, the strain rate increases and becomes, for a transient, higher than the nominal strain rate, and in the third stage the strain rate is again constant and equal to the nominal one. The experimentally measured displacement of both sample and motor during a typical test as well as the stress are shown as a function of time in Figure 12.

One can note that the sharp increase in strain rate (or, in other words, the acceleration of the displacement) corresponds to a drop in the measured force. This point was also noted and discussed in detail for fluid layers [26,30]. In the context of an adhesively bonded layer, however, the drop in force does not correspond to any fluid flow but to the adhesive detachment of the layer from its substrate.

Simple Model of Equivalent Springs

The apparatus and the elastic layer can be considered as two springs in series.

A total displacement, Δ, is applied to the entire assembly. At first, both springs extend but the degree of extension directly depends on

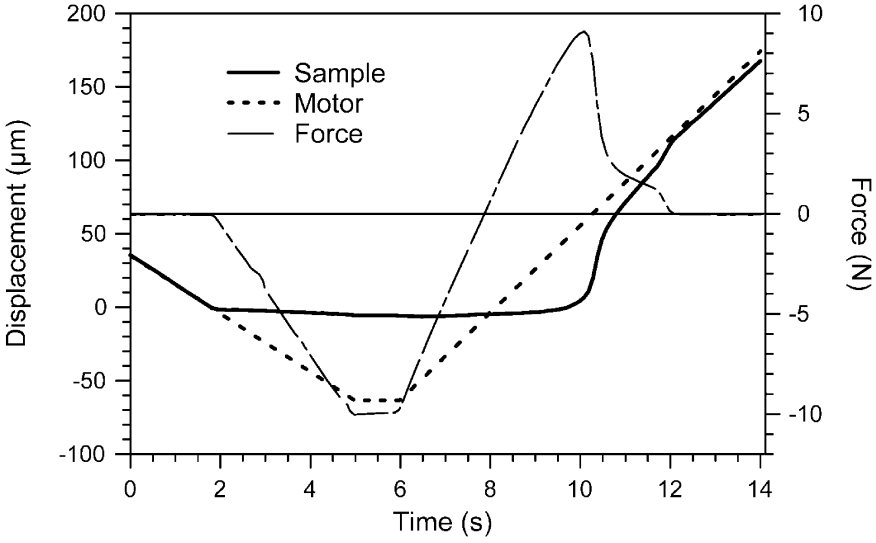

FIGURE 12 Motor and Sample displacement (left scale) and Force (right scale) as a function of time during a probe test. Note the very different levels of compression to which the apparatus and the sample are subjected.

the relative compliance of the springs. Since forces are transmitted through the apparatus, one can write

$$F = \frac{\delta_s}{C_s} = \frac{\Delta - \delta_s}{C_m}, \tag{A2}$$

where F is the force; δ_s and Δ are the displacements of the sample and of the motor drive, respectively; and C_m and C_s the compliances of the apparatus and of the sample, respectively. Rearranging Equation (A2) one obtains

$$\delta_s = \frac{\Delta \cdot C_s}{C_s + C_m} \tag{A3}$$

and

$$\frac{d\delta_s}{dt} = \frac{\cdot V_{nom} \cdot \left(C_s(C_s + C_m) + \frac{dC_s}{dt} \cdot t\right)}{(C_s + C_m)^2}, \tag{A4}$$

where V_{nom} is the nominal probe velocity. Therefore, the rate of displacement that the sample sees, $\mathrm{d}\delta_s/\mathrm{d}t$, or in other words the rate at which the two plates are separated, $\mathrm{d}h/\mathrm{d}t$, is only constant in two limiting cases: in the case where C_s is constant and in the case where

$C_s \gg C_m$, which is equivalent to a very stiff machine. In all other cases $\mathrm{d}h/\mathrm{d}t$, and therefore the rate at which external work is performed on the adhesive layer, is not constant. While this is not important if the failure of the layer is fully elastic, it becomes very important if the failure process is viscoelastic.

Let us now examine the implication of taking the compliance into account for the force-displacement curves. In the beginning of the detachment process, as one can see in Figure 12, the force increases linearly with the displacement of the drive, Δ. Since Δ is set as $\Delta = V_{nom}$, this result indicates that the compliance of the sample (C_s) is constant during this stage. However, because of the contribution of the machine the average displacement rate that the layer sees is not V_{nom} but is given by:

$$\frac{d\delta_s}{dt} = \frac{C_s \cdot V_{nom}}{C_s + C_m} \tag{A5}$$

It is clear here that $d\delta_s/dt$ is always lower than V_{nom} unless the stiffness of the apparatus is very large.

Corrected Force-Displacement Curves

The characteristic force-displacement curve of the adhesive layer is not $F(\Delta)$, where Δ is the total displacement of the drive, but $F(\delta_s)$.

Figure 13 shows the raw and corrected force-displacement curves for a typical probe test. As one can readily see, since the apparatus is here rather compliant, the compliance correction significantly changes the shape of the force curve.

Furthermore, each point in the corrected force-displacement curve does not correspond to the same value of $d\delta_s/dt$. In the beginning of the test, the sample hardly deforms and the corresponding strain rate that the sample sees is very low. At the end of the test, the sample deforms significantly while the apparatus is hardly deformed. In this regime $\Delta = \delta_s$ and the test is, indeed, performed in displacement control.

Let us examine the consequences of this behavior on the results obtained: For a nonstop test, the adhesion energy can be measured as the integral of the force over the motor displacement, Δ, or over the sample displacement, δ_s. This is qualitatively seen in Figure 13 and can be more quantitatively shown by the following argument.

The work of debonding measured from the nominal displacement is

$$W_n = \int_0^{\Delta} F \cdot d\Delta, \tag{A6}$$

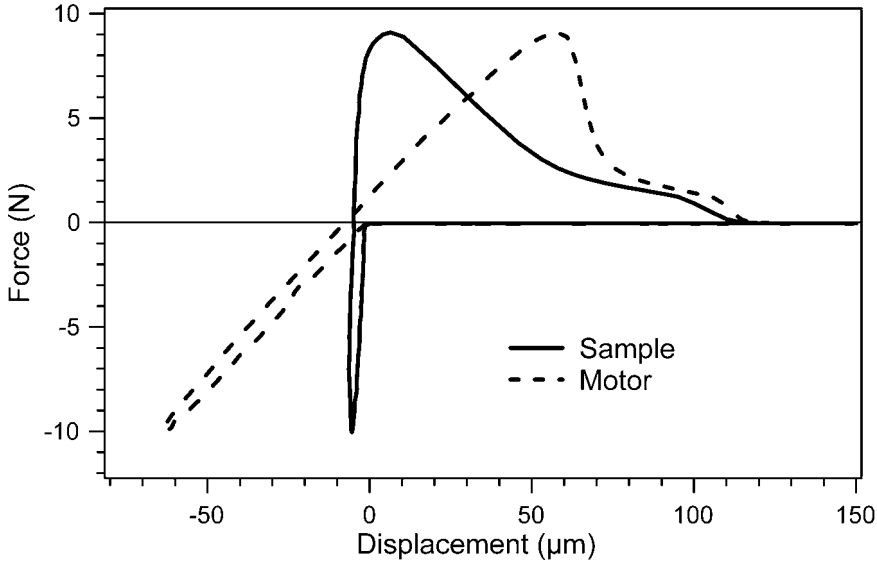

FIGURE 13 Same force-displacement curve as a function of motor displacement and adhesive displacement.

while the work of adhesion measured from the sample displacement is

$$\begin{aligned} W &= \int_0^{\delta_f} F \cdot d\delta_s \\ &= \int_0^{\delta_f} F \cdot d(\Delta - FC_m) \\ &= \int_0^{\delta_f} F \cdot d(\Delta) - C_m \cdot \int_{F(\delta=0)}^{F(\delta_f)} F \cdot dF, \end{aligned} \tag{A7}$$

where the subscript f stands for "final." Since $F(\delta_f) = 0$, the first integral is equivalent to W_n and the second integral is zero. Therefore $W_n = W$. This last equality is, of course, only true if the integral of the energy is done between two points where the force is zero.

However, the actual value of the integral may depend on the compliance of the apparatus. In the intermediate regime where the compliance of the sample changes rapidly, crack propagation and apparatus compliance are closely coupled. The apparatus acts as an

energy reservoir, which is suddenly emptied during the compliance change. Therefore, the more compliant the apparatus is, the larger the reservoir and the faster the energy dissipation during the detachment of the adhesive from the surface. This will result in a higher apparent work of adhesion.

If the interfacial crack propagation follows a classic relationship of the type given in Equation (1), a detailed simulation of the detachment of the adhesive can be performed along the same lines as that done in Barquins and Maugis [29]. Such a simulation is in qualitative agreement with the behavior described above. However, because of significant differences between the assumptions of the simulation (propagation of an annular crack, infinitesimal deformations), it requires a separate and rather detailed discussion which goes beyond the scope of this article and will be the subject of a forthcoming paper.